

Results of the application of persistent scatterers interferometry for surface displacements monitoring in the Azul open pit manganese mine (Carajás Province, Amazon region) using TerraSAR-X data

Carolina de Athayde Pinto, Waldir Renato Paradella, José Claudio Mura, Fabio Furlan Gama, Athos Ribeiro dos Santos, Guilherme Gregório Silva
National Instituto for Space Research (INPE), São José dos Campos, São Paulo State, CEP 12227-010, Brazil

ABSTRACT

Brazil has 10% of global Mn reserves with its most important mine located in the Amazon region. The Azul deposit is related to sandstones and siltstones of the Águas Claras Formation (Archean), situated in the central portion of the Carajás Strike-Slip System. Vale S.A. mining company operates the Azul mining complex with three simultaneous excavations (mines 1, 2 and 3) conducted on rock materials of low geomechanical qualities. Mining operations are open-pit, with 4-8 m-high benches and depth of 80 m. A stack of 19 TerraSAR-X (TSX) images was used for the investigation covering the period of March 20-October 4, 2012. In order to minimize the topography phase error in the interferometric process, a high resolution DEM was generated based on a panchromatic GeoEye-1 stereo pair. Persistent Scatterers Interferometry (PSI) analysis was carried out using the IPTA (Interferometric Point Target Analysis) software and led to the detection of 40,193 point-wise persistent scatterers (PS), with an average density of 5,387 PS/km². It was concluded that most of the mining area can be considered stable during the TSX coverage. High deformation rates related to settlements were mapped over a waste pile, while small deformation rates were detected along the north and south flanks of mine 1 and were interpreted as cut slope movements toward the center of the pit. Despite only ground-based radar measurements were available for a short time period during the TSX coverage, and covering a sector of bench walls along the south flank of mine 1, the PSs movement patterns showed concordance with the field measurements. The investigation emphasized the important role that PSI technique can play in planning and risk assessment in this mining area. Monitoring of this type of deformation by PSI can usefully complement other commonly used field geotechnical measurements due to the synoptic SAR coverage over a dense grid, providing ground deformation data independently of field access and with millimeter accuracy.

Keywords: persistent scatterers interferometry, TerraSAR-X, Azul open pit manganese mine, Brazilian Amazon region

1. INTRODUCTION

Brazil has 10% of global Mn reserves, after Ukraine (24%), South Africa (22%) and Australia (16%). Vale S.A. is the largest Mn producer in Brazil, accounting for 70% of the country's market. The Azul complex, located in the easternmost border of Brazilian Amazon region, encompasses the most important Brazilian Mn mine, with a production of 1,850 Mt in 2013¹.

Instabilities can be expected at any mining activity. The open pit operations usually have significant areas of extent and can also influence large portions of terrain adjacent to the pit crest. Surface deformations and rock mass movements potentially lead to slope instabilities or wall failures due to regular open pit mining operations. The eventual collapse of slopes can cause loss of equipment, risk to personnel and infrastructure, disrupting mine scheduling with an increase in production cost. This scenario in Carajás gets worse over time due to intense excavations in rock alteration products of very low geomechanical quality, coupled with heavy precipitation of the moist tropics. It is worth noting that small

surface movements on a mine highwall may be precursors of a failure². Thus, an effective prediction and management of mining induced deformations of ground surface should be a key concern for the mining industry.

Most major open pit mines employ geotechnical teams to frequently monitor ground movements and data on surface stability have traditionally been collected through the use of deformation measurements. A detailed classification scheme of the available monitoring systems for open pit mines was recently presented³. In this scheme, ground displacement measurement techniques were divided into surface measurements at discrete points with specific instruments (total stations/ prisms, extensometers, GNSS, etc.), and surface measurements over areas based on scanning (ground-based radar, Laser) and image techniques (photogrammetry, etc.) It is important to consider that systems that monitor deformation over large areas yield distinct information when compared to systems designed for monitoring restricted sectors or selected points, since the former can provide valuable data about the spatial patterns of deformation. Thus, scanning ground-based radar such as the slope stability radar (SSR)⁴, which monitors deformation quasi-continuously, is considered "a real-time technique" and is widely used by the majority of open pit mines for operational safety. Its rapid response and area coverage are ideal attributes for monitoring slope stability during mining operations. Lower cost monitoring instruments such as total station/reflecting prism and extensometer are normally used for background monitoring of benches/berms, but once instability has been detected, SSR is the instrument of choice, such as in Carajás⁵. However, even though SSR has the ability to cover a broad area, the deformation monitoring is still restricted to sectors of the pit. Since large open-cut mining encompasses significant areas of extent with a great demand of land movement information, within and beyond the pit limits (stock and waste piles, tailings ponds, dams, transport routes, processing facilities, mine infrastructure, etc.), the use of Differential Interferometric Synthetic Aperture Radar (DInSAR) for monitoring purpose is justified, particularly due to the versatility of systematic all-weather data acquisition through satellite systems. The basic advantages of DInSAR over total station/reflecting prisms or ground-based radar techniques are that measurements of the spatial movement patterns can be made without fieldwork and detailed motion information (millimeter scale) can be acquired over large areas. However, according to⁶ four main problems have limited the use of DInSAR on a fully operational basis: (1) temporal decorrelation of surface scatterers due to surface changes process, (2) spatial decorrelation due to the large baseline between SAR acquisitions, (3) atmospheric effects causing variation in signal delays and (4) resolving phase ambiguity.

In order to overcome the problems mentioned above, PSI technique is a recent alternative based on the usage of long time series of interferometric SAR image which allows for millimetric precision ground deformation mapping⁷. Many successful PSI results can be found in the literature related to underground mines (⁸⁻¹⁷), with few papers to open pit environments (¹⁸⁻²⁰). The complexity of the Azul mining complex makes PSI a challenging application for displacements monitoring. The mining activities are characterized by excavations in thick lateritic cover (saprolitic soils) and rock alteration masses showing low geomechanical qualities, by heavy rainfall periods, and a highly dynamic surface changes due to constant reworking and removal of materials, all contributing to an overall loss of radar coherence. In this paper, we report the first results of the application of PSI for mapping ground displacements within and around the Azul open pit mine using TSX data. The results were compared with information provided by Vale S.A., represented by SSR surface measurements along bench walls. The result achieved was very satisfactory as it was possible to obtain synoptic and detailed ground displacement information at good accuracy, as confirmed by initial comparison with in-situ measurements.

STUDY AREA

The Azul deposit, located within the Carajás Mineral Province, was discovered in September 1971, and started the mining activities in 1985, with Mn reserves of 45.4 Mt @ 40.5% proven, and 8.3 Mt at 39.5% probable (December 2011). It is recognized internationally for the excellent quality of its ore, which contains high concentrations of Mn and a high Mn-Fe ratio. Now spanning three simultaneous mines (1, 2 and 3) and a processing plant, the Azul Complex operations are open-pit, with benches of 4-8 m high and 5m width, and depth of 80 m. Its production reached 1.850 million tons in 2013 and focuses on metallurgical Mn and Mn dioxide (Figure 1). A large waste pile is also located along the northern border of mine 1. This manmade mining structure with 20 years age is a heaped-fill dump configuration, with 10 m bench height, 10 m berm width, and 27⁰ of overall slope angle (crest-to-toe).

The Azul deposit is related to the Proterozoic Águas Claras Formation, which is characterized by a progradational succession of platform sediments in the lower part and littoral and fluvial deposits in the upper part²¹. The primary mineralization is hosted in a pelitic sequence on the basal portion of this unit, and the secondary mineralization, which is considered the most important, is related to residual/supergene enrichment associated with mature lateritic toposequence acting from at least Upper Cretaceous throughout the Tertiary and Quaternary. The geologic sections exposed in the mining area show the dominance of fine red to white sandstones and siltstones/pelites, that include lense-form layers made of gray siltstones to gray black shales, rich in carbonaceous organic matter and/or Mn oxi-hydroxides (OH-Mn) or rhodocrosite, characteristics of terrigenous/chemical and lateritic sources. Primary structures such as hummocky cross stratification and parallel laminations are common in these rocks. Bedding with thickness of centimeters to a few meters (30-50 cm) represents the main primary structure. The lateritic profile is deep (100 m) and is characterized by horizons, which correspond to progressively upward physico-chemical degradation from a thick clayey horizon to nodular lateritic crust, breccia-like, cavernous or massive. Large sectors of the mining area are covered by yellowish brown earthy to clayey material, with spheruliths concentrated at the base as products of chemical and physical weathering of the lateritic profile, and deposited by gravity in paleodepressions or paleovalleys²².

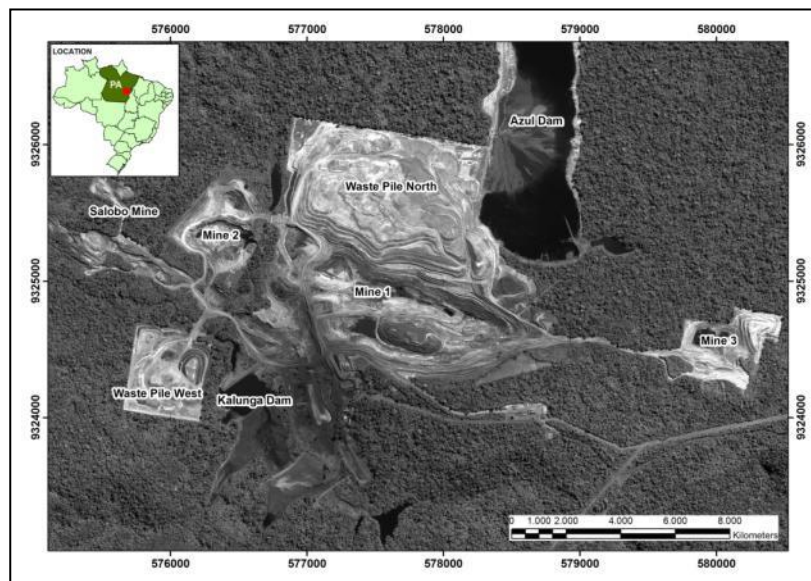


Figure 1. Azul mining Complex with three simultaneous active open pits (mines 1, 2, 3), two waste piles and mining infrastructure.

Structurally, the Azul deposit is located in the central portion of the Carajás Strike-Slip System (CSSS) and the rocks in the area are organized in asymmetric folds cut by N-S trending normal faults and by E-W trending directional/thrust faults. The parallelism of the structural trends in the deposit and lineaments related to the CSSS suggests a close relation with regional deformation (dextral transtensional and sinistral transpressional episodes). Faults with normal kinematics associated to dextral component of displacement are the major exposures in the area and are interpreted as related to transensional episodes of the installation of the Carajás Fault prior to 2.6 Ga. Folds, thrust faults and sub-vertical fault zones would be related to deformations under sinistral transpressional regime, a second event responsible for the reactivation and tectonic inversion of most of the primary structures near the Carajás Fault zone²³.

The most detailed available account of the geological and geomechanical information for the Azul Complex was produced by Vale’s geotechnical team, including surface outcrop mapping at 1: 2,000 scale, classification of rock types based on standard mining nomenclature, characterization of structural and geomechanical parameters and definition of lithostructural domains restricted for slopes of mine 1²⁴. Furthermore, a slope stability analysis was also carried out, which involved the collection of structural data, slope geometry and subsequent limit equilibrium analysis in order to

characterize conditioning structures of slope ruptures. Based on this report, rock types and alteration products were characterized with variations in the degree of weathering and strength, but with a dominance of types with poor mechanical properties. The integration of geological and geomechanical information is presented in Figure 2. Based on the field mining nomenclature, the lithotypes were classified as siltstones, argillites, silty manganeseiferous pelites, massive Mn ore, rich Mn tear pelites and pisolites. A lateritic detritic cover and argillaceous soils are also common. The geotechnical quality of the rock masses was evaluated based on RMR parameter ratings according to ²⁵ and poor and very poor classes are dominant, while good rock masses crop out as isolated bodies. Two main structural features were mapped in mine 1 (notation dip direction/dip): (a) beddings with two dominant attitudes (36/207 and 43/016), (b) fractures/faults with four attitude systems (71/43, 69/129, 67/224 and 68/311). Finally, the kinematic analysis has pointed out the possibilities of distinct failures (plane, wedge, circular and toppling) along sectors of cut-slopes of pit 1. Since the detailed information is related to mine 1, the PSI analysis was restricted to this area.

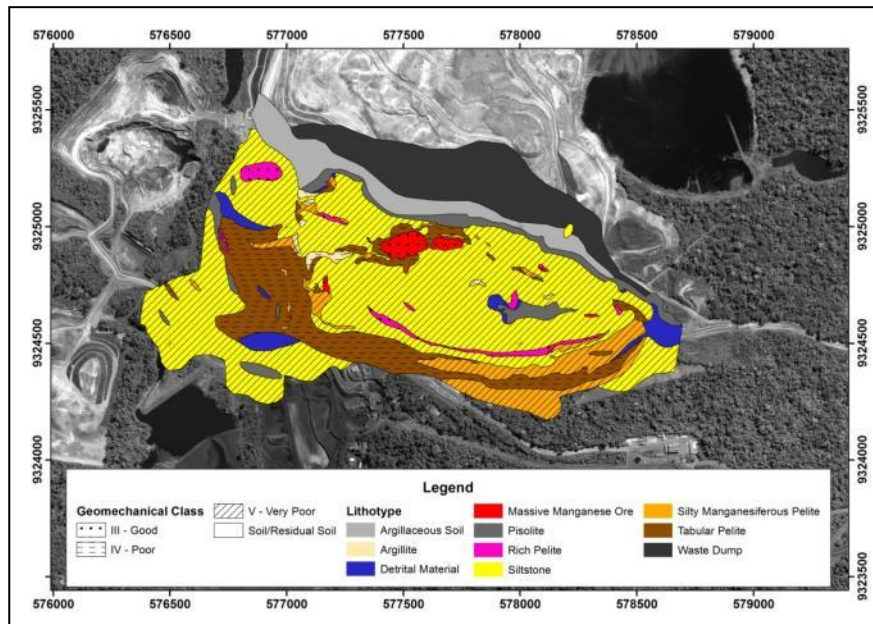


Figure 2. Lithological and geomechanical units in mine 1.

2. DATASET

A stack of 19 TSX Strip Map images (repeat cycle of 11 days) was used for the investigation covering the dry season (March 20-October 4, 2012) in the area. The SLC images were acquired under ascending passes (look azimuth = 78 degrees), incidence angle range of 39.89 - 42.21°, spatial resolution of 1.7 m x 3.49 m (rg x az), pixel spacing of 1.36 x 1.90 m (rg x az), and width swath of 30 km. In order to minimize the topography phase error in the interferometric process, a high resolution DEM was generated based on a panchromatic GeoEye-1 stereo pair. The GeoEye stereo images were acquired on July 1st, 2012. The first scene was collected with nominal azimuth and elevation angles of 29.4 and 82.4°, whereas the second scene was acquired with azimuth and elevation angles of 187.42 and 62.20°, respectively. The images were provided with 0.5 m spatial resolution and RPCs (Rational polynomial coefficients). The generation of the DEM was based on OrthoEngine PCI Geomatics through the Rational Function Method (RFM) as the geometric model. The panchromatic DEM was produced at 2m spacing using, and its elevation values compared to seven well-defined accurate vertical check points have provided RMS and maximum errors of 1.2m and 1.6m, respectively ²⁶.

The slope monitoring scheme used by Vale in Carajás includes regular visual inspections to detect the onset of instability and instruments measuring surface (total station/reflecting prisms and ground based radar) and subsurface displacements (piezometers, extensometers). Only information produced from the ground based radar SSR was available for this investigation. Slope stability monitoring radars use a phase measure, similarly to the interferometry technique, to infer

small changes in range (i.e., in the Line-of-Sight direction toward the radar) associated with pre-cursor movements to mine slope failures. These small changes in phase are accumulated over time for each subsequent scan and converted to displacement values. SSR features a 1.80 m-diameter scanning parabolic dish antenna, mounts, controlling/data-collecting computer, remote area power supply, warning siren and lights, CCD camera, communication links, and Internet compatibility. The system uses real aperture radar to scan a slope both vertically (height) and horizontally (azimuth) with a scanning at a rate of 10^0 /sec over a range of $\pm 60^0$ vertically and 270^0 horizontally. Typical scan repeat time is 15 min. Line-of-Sight (LoS) displacement can be measured to ± 0.2 mm without the use of reflectors. For the configuration used in the Azul complex, the SSR pixel size was roughly 1.7 x 1.7 m. The SSR data corresponded to measurements taken on bench walls located along the mine 1, and covered a short time span (August 03-08, 2012). A small deformation pattern was detected, which was not considered relevant to cause significant ruptures in the slopes²⁷.

3. PERSISTENT SCATTERERS INTERFEROMETRY AND METHODOLOGICAL APPROACH

The PSI approach used in this study relies on identifying pixels whose scattering properties vary little with time and look angle in a stack of co-registered SLC images. The idea of PSI is to analyze the temporal and spatial characteristics of the interferometric phase of individual point targets. These point targets are coherent even for the interferometric pairs with long spatial baselines and remain stable over long time periods to permit analysis of the phase history (²⁸⁻³⁰).

PSI analysis was carried out using the IPTA (Interferometric Point Target Analysis) software, which is the implementation of PSI by GAMMA Remote Sensing and Consulting AG (GAMMA). The IPTA software is a toolbox that can support many different methodologies including different alternatives for scatterers candidate selection, spatial and temporal phase unwrapping, and supporting approaches for single as well as multireference stacks³¹. The overall processing using IPTA is depicted on Figure 3. The processing sequence included SAR SLC image co-registration to generate the stack of interferograms (the master scene was selected based on a configuration that presented low perpendicular baseline dispersion and near to center of the temporal acquisition sequence, Table 1), stack of differential interferograms generation, point target candidate determination (based on spectral phase diversity and low intensity variability), interferometric point analysis based in two-dimensional regression (phase model indicates a linear dependence of the topographic phase on the perpendicular baseline and also indicates a linear time dependence for deformation rates) and model refinement (update the DEM, update the deformation rates, baseline refinement). An important aspect of IPTA is the possibility of a step-wise, iterative improvement for different parameters, such as the topographic error based in a linear regression with the perpendicular baseline set and the linear regression for deformation estimation. The residues of this last regression containing the atmospheric phase, which is related to the path delay heterogeneity at the two acquisitions times of the pair, as well as non-linear deformation and noise, were spatially and temporally filtered to decrease the atmospheric phase delay and noise, as well as to retrieve the non-linear deformation component.

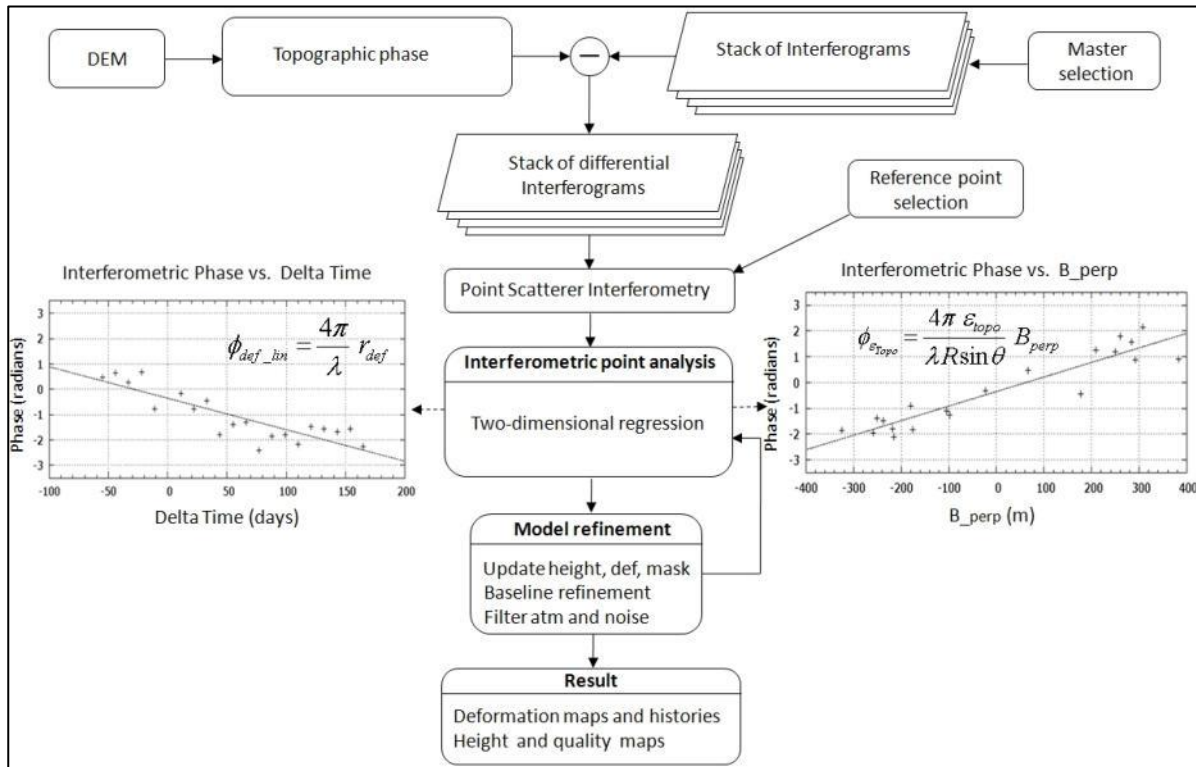


Figure 3. Flow diagram outlining the IPTA processing sequence.

Table 1. Interferometric TSX pairs selected for PSI processing.

Master	Slave	Temporal baseline (days)	Perpendicular Baseline (m)
2012/07/08	2012/03/20	-110	79.39
2012/07/08	2012/03/31	-99	-82.80
2012/07/08	2012/04/11	-88	-140.96
2012/07/08	2012/04/22	-77	411.41
2012/07/08	2012/05/03	-66	-119.80
2012/07/08	2012/05/14	-55	98.88
2012/07/08	2012/05/25	-44	386.88
2012/07/08	2012/06/05	-33	-6.547
2012/07/08	2012/06/16	-22	-228.91
2012/07/08	2012/06/27	-11	487.23
2012/07/08	2012/07/19	11	-163.87
2012/07/08	2012/07/30	22	279.61
2012/07/08	2012/08/10	33	394.86
2012/07/08	2012/08/21	44	-120.72
2012/07/08	2012/09/01	55	-78.20
2012/07/08	2012/09/12	66	-154.28
2012/07/08	2012/09/23	77	309.99
2012/07/08	2012/10/04	88	166.72

4. RESULTS AND DISCUSSIONS

IPTA PS points were detected and their displacement rates expressed by average velocities computed with millimeter precision for the monitored period. Positive values correspond to motion toward the satellite; negative values correspond

to motion away from the satellite (mm/yr). For each measurement point, the (mean) annual LoS velocity and the displacement temporal series were calculated relative to a reference point assumed stable (location UTM 22M 577255.375E 932402.000N). The IPTA analysis performed with 19 TSX scenes has allowed the detection of 40,193 PS, with an average density of about 8,588 PS/km² (Figure 4). The distribution of PS was not homogeneous: no stable targets were present on vegetated areas, while the coverage of PS was very good over the mining activities areas (within and beyond the pit limits, waste piles, processing facilities and mine infrastructure). It was concluded that most of the mining area can be considered stable during the TSX coverage (yellow-greenish regions), and the number and distribution of PS provided a powerful unique view of the stability conditions going on in the searched areas of the mine 1.

The highest deformation rates (yellow-reddish regions) indicative of settlements were mapped over the north waste pile (Figure 4, letter A), with deformation rate and LoS accumulated subsidence reaching -17.02 cm/year and -8.65 cm, respectively. Waste material settlements occur due to several causes such as particle reorientation, weathering of high clay-content materials, presence of water in inter-particle bounding, and transport of particles through the dump. During construction a higher settlement rate may occur followed by lower vertical deformation at a decreasing rate, and have been shown to continue 10 years or more after the pile construction. The rate of settlements of waste dumps is a controversial issue in the literature, since it depends on several parameters (dump height, dump type, loading rate, type of material, dump construction time, etc.), with large variations of settlements (0.3 up to 20%) regarding the waste dump height being reported³², but on general, vertical settlements of few meters are normally expected. Thus, the LoS accumulated values are within the expected limits (Figure 5). Furthermore, it is also important to mention that it was not detected sectors of ground displacements with positive values characterized by bulging at the dump toe indicative of pile instabilities. Finally, it is also clear by the low presence of PS for the waste pile, that this manmade structure has suffered intense surface changes due to ongoing mining operation expressed by the low SAR coherence.

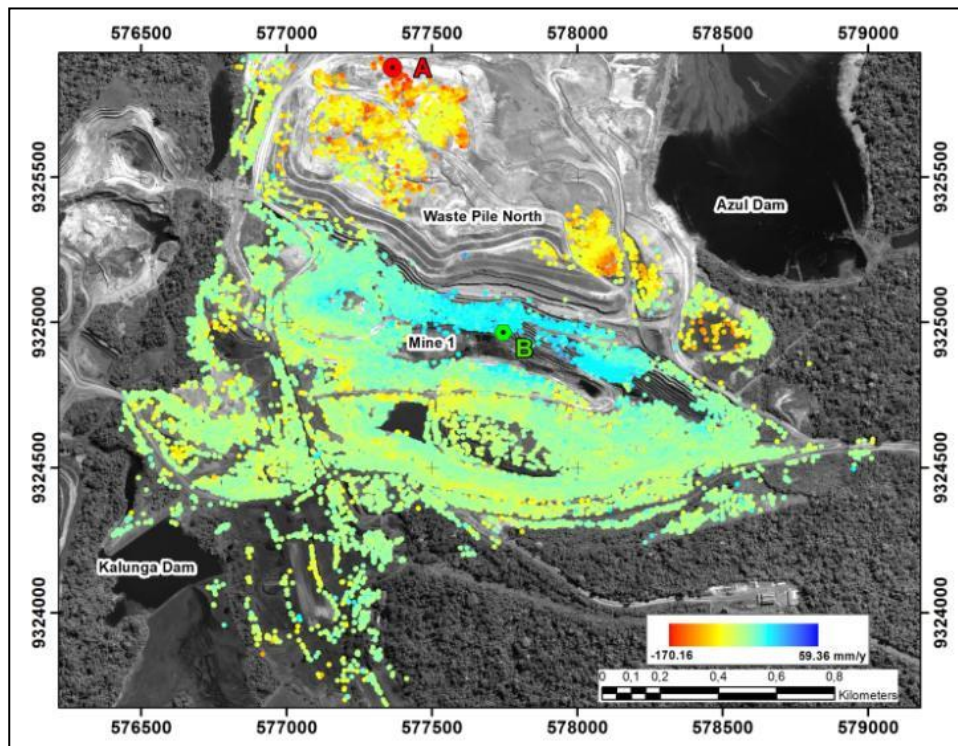


Figure 4. Spatial distribution of PS for mine 1 and north waste pile, visualized by the average LoS velocity on the Panchromatic GeoEye image.

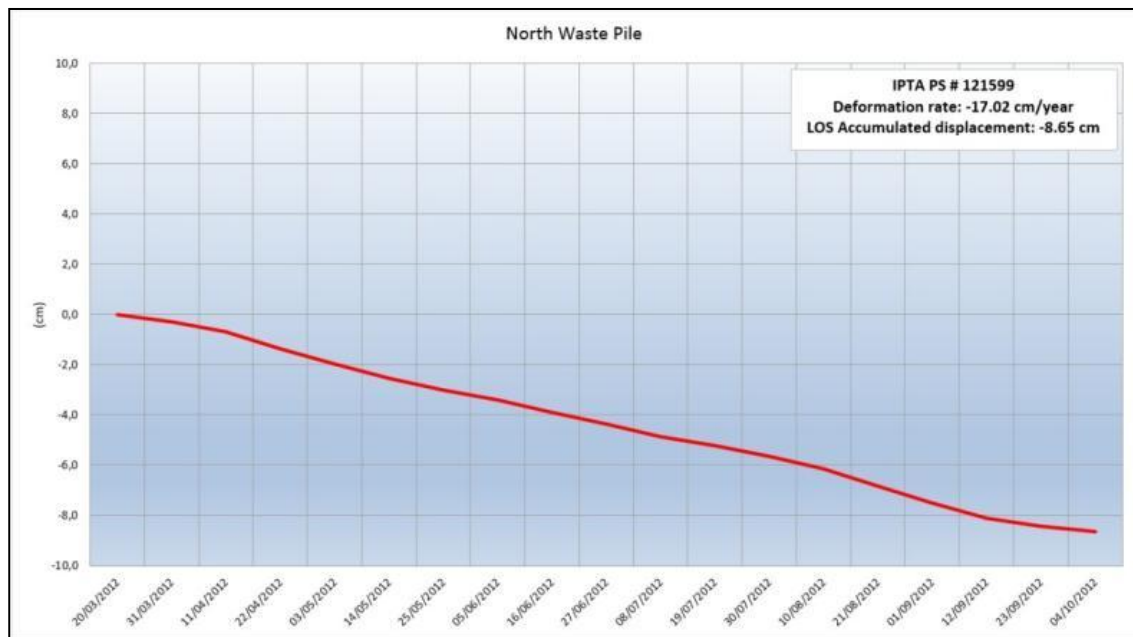


Figure 5. Displacement history during the period of March 20-October 04, 2012 for the IPTA PS # 121599 (letter A, Figure 4) showing subsidence due to settlements of the north waste pile.

Ground displacements were also detected for cut slopes along the northern flank with positive values indicative of movement towards the sensor (bluish regions) showing values for deformation rate and LoS accumulated displacement of 4.67 cm/year and 2.41 cm, respectively (Figure 6). In an attempt to validate the PSI results with field surface displacements, SSR measurements, restricted to the monitoring of pit walls along the south flank, were used. Despite of the short field monitoring period (03 up to 08 August, 2012), a small deformation pattern given by successive small collapses followed by stabilizations was detected, with a maximum accumulated LoS-projected SSR deformation value of 15 mm (Figure 7).

Under an ArcGis environment, the distinct viewing geometries for the SSR and TSX were superimposed on the panchromatic GeoEye orthoimage in order to explore spatial relationships (Figure 8). It can be seen in this figure that the look directions for both imaging radars (orbital and ground based) are almost orthogonal. Thus, the measured motion component along the SSR LoS would be attenuated when projected to the TSX LoS, since no significant phase variation is detected if the terrain is affected by displacements in the direction perpendicular to the sensor LoS. Figure 9 shows the LoS-projected TSX deformation profiles for three points (A, B, C) specially located along the SSR look azimuth (from bottom to the top) of the benches of south flank. The PS profiles revealed the presence of slope displacements indicative of LoS range lengthening with small rates, increasing from the bottom to the top of the benches (point A = -0.37 cm/year, point B = -0.70 cm/year, point C = -4.21 cm/year). Point B is almost in the same location where the SSR profile was acquired with a total accumulated displacement of 15 mm for the six-day field monitoring period. The direct comparison of deformation values measured by both systems is not feasible due to distinct aspects (sensor viewing geometry, bench faces measurement with SSR and bench floors/berms with TSX, time-scan, etc.). However, they are concordant regarding the presence of small movements along the cut slopes.

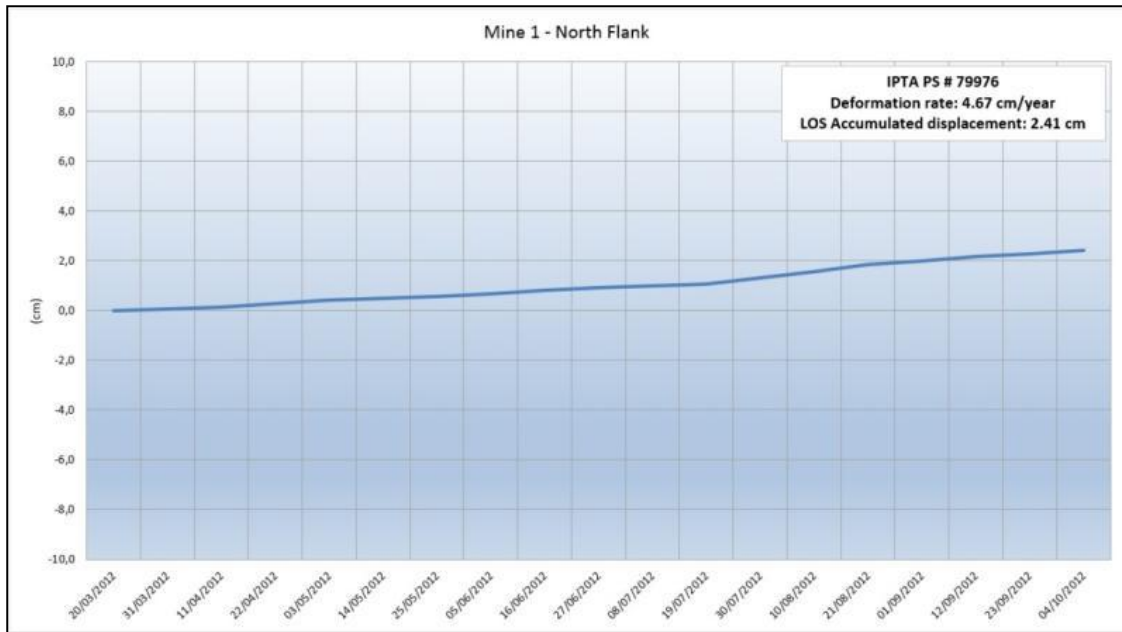


Figure 6. Displacement profile related to the period of March 20-October 10, 2012 for the IPTA PS # 79976 (letter B, Figure 4) showing movement towards the SAR along the cut slopes of north flank of pit 1.

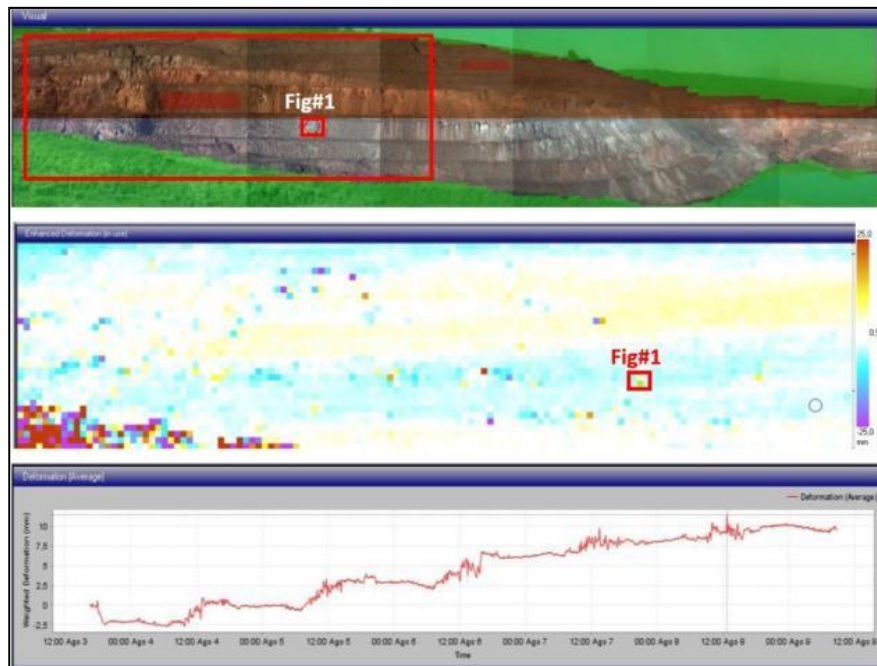


Figure 7. LoS-projected SSR deformation plot showing the photograph of the scanned area (top); corresponding "heat map" deformation of the scanned area with color scale representing lower to higher LoS-projected SSR displacement variation (middle); deformation profile for the selected area (rectangle) with small collapses followed by stabilization (bottom).

It is worth noting that the deformation rates provided by TSX with LoS range lengthening (away from the satellite) along pit walls of south flank and LoS range shortening (towards the satellite) along pit walls of north flank suggest motion components aligned toward the center of the pit 1. Furthermore, the small deformations that were measured in the field are aligned along the SSR LoS roughly oriented in the north-south direction due to the viewing geometry acquisition of the ground based radar. This field displacement could represent the north-south component of the overall small slope movement trend toward the center of the pit 1 for the south flank. Taking into account that the geotechnical evaluation carried out by Vale S.A. is conclusive regarding the absence of major instabilities in this sector that could lead to large scale movement and eventual failure, the PS deformation patterns are interpreted as normal deformations responsive to the open pit mining operations, characterized according² to stress relaxation of slopes due to pit excavation and the confinement provided by the rock mass has been lifted. However, more specific works are required to assess the role of other important components in the detected deformation patterns (lithology, structures, geomechanical classes, groundwater flux, slope design, etc).

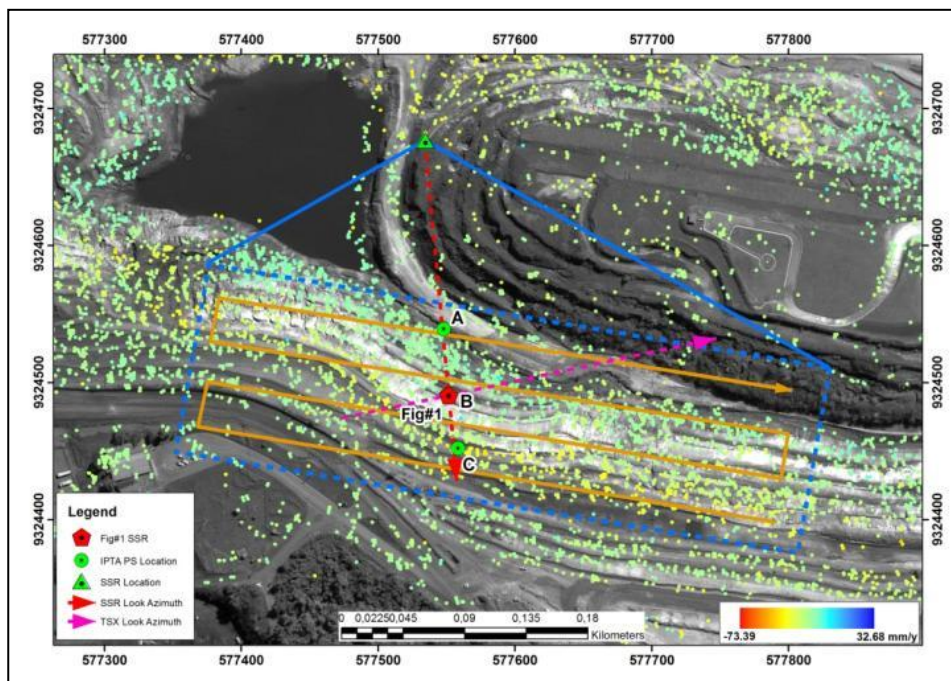


Figure 8. Scheme of viewing geometries used by TSX and SSR during the monitoring of benches along the southern slopes of Pit 1. Legend: TSX look azimuth (magenta), SSR look azimuth (red), SSR location (green triangle), points A, B, and C along SSR look azimuth are discussed in the text. Point B corresponds to the same location where the SSR deformation plot was produced (rectangle in Figure 7).

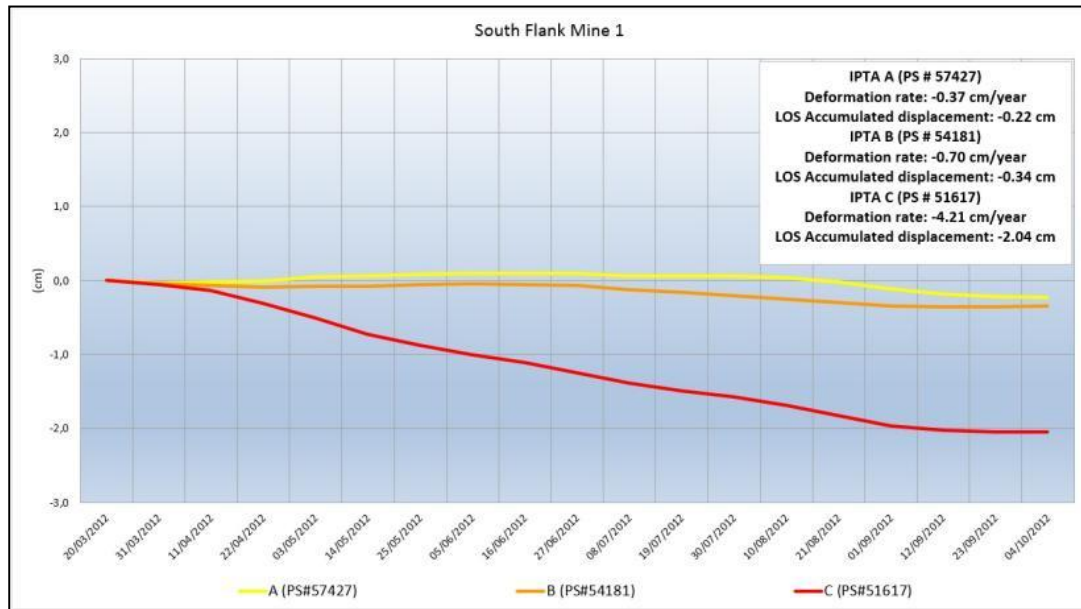


Figure 9. LoS-projected TSX displacement profiles for three PS (A, B, C) located along the SSR look direction from the bottom to the top of monitored bench walls of Pit 1 (south flank).

5. CONCLUSIONS

PSI analysis using a stack of 19 TSX images was applied to measure surface displacements in the Azul complex for the period of March 20-October 04, 2012. The approach has provided a synoptic view of the ongoing deformative processes in the searched area. The deformation rate map showed that most of the mine 1 area, including the infrastructure, was stable during the time span of the TSX coverage. A deformation rate reaching -17.02 cm/year was related to a waste dump and was interpreted as normal expected settlements with no evidences of pile instability. Ground displacements were also detected for bench floors and berms along the north and south flanks of pit 1, with movements toward the satellite (deformation rate of 4.67 cm/year) and away the satellite (deformation rate of -4.21 cm/year), respectively. They are indicatives of a general sense of movement toward the center of the pit during the TSX coverage, probably caused by the mining activities (unloading responses). Although it was not possible to directly compare the total amount of subsidence measured by spaceborne SAR with the field measurement by ground-based radar, the results showed concordance regarding the presence of small movements along the cut slopes for almost the same location. This confirms that PSI may be used for mining monitoring and risk assessments, providing data with high accuracy of displacements, over a dense grid and a large area. In order to fully exploit the potentiality of PSI approach, the usage of ascending and descending SAR passes is necessary in order to complement the viewing geometry, minimize lack of information in the case of acquisition failures, and also to get horizontal and vertical deformation components. A complementary and synergistic use of space-based SAR information with field monitoring system information proved to be fundamentals for operational perspective. The next step of investigation will focus on the assessment of TSX images of the wet season, which is considered the most critical period in the area for stability.

ACKNOWLEDGEMENTS

This investigation was carried out under the scope of the FAPESP-Vale-INPE project (FAPESP proc. # 2010/51267-9). The authors would like to thank Vale S.A. for providing access to geological, geomechanical and in situ ground deformation data (SSR). The National Council for Scientific and Technological Development (CNPq) are also

acknowledged for grants received by the first and second authors during this investigation. The authors are particularly grateful to the Geotechnical Vale's team in Carajás for the support during the field campaign.

REFERENCES

- [1] Vale S.A. "2013 and 4Q13 Production Report", Vale S.A. Mining Company, Rio de Janeiro, <http://www.vale.com/EN/investors/Quarterly-results-reports/Quarterlyresults/PREPORT4T13_i.pdf>(26 June 2014) <http://www.vale.com/EN/aboutvale/Pages/default.aspx>.
- [2] Read, J. and Stacey, P. [Guidelines for open pit slope design], CSIRO publishing, Australia, (2009).
- [3] Vaziri, A., Moore, L., and Ali, H. "Monitoring systems for warning impending failures in slopes and open pit mines", *Natural Hazards*, 55, 510-512 (2010).
- [4] GroundProbe. "The Slope Stability Radar (SSR): ground breaking making mining safer", may 2014 News, Australia <[http://www.groundprobe.com/CMS/Plugins/LatestNews/files/1402534476-GroundProbeNewsletter-May-2014-\(English\).pdf](http://www.groundprobe.com/CMS/Plugins/LatestNews/files/1402534476-GroundProbeNewsletter-May-2014-(English).pdf)>(26 June 2014) <http://www.groundprobe.com/products-and-services/slope-stability-radar-ssr>
- [5] Nader, A. S. "Slope monitoring through slope stability radar as a key performance indicator of geotechnical development integrated with primary activities of mineral value chain". Doctoral Thesis in Mineral Engineering, Politechnical Scholl, São Paulo University, original in Portuguese (2012).
- [6] Ferretti, A., Prati, C., and Rocca, F. "Nonlinear Subsidence Rate Estimation Using Permanent Scatterers in Differential SAR Interferometry", *IEEE Transactions on Geosciences and Remote Sensing*, 38 (5), 2202-2212 (2000).
- [7] Ferretti, A., Prati, C., and Rocca, F. "Permanent Scatterers in SAR Interferometry", *IEEE Transactions on Geosciences and Remote Sensing*, 39 (1), 8-20 (2001).
- [8] Colesanti, C., Mouelic, S. L., Bennani, M., Raucoules, D., Carnec, C., and Ferretti, A. "Detection of mining related ground instabilities using the Permanent Scatterers technique: a case study in the east of France", *International Journal of Remote Sensing*, 26 (1), 201-207 (2005).
- [9] Jung, H.C., Kim, S. W., Jung, H. S., Min, K.D., and Won, J.S. "Satellite observation of coal mining subsidence by persistent scatterer analysis", *Engineering Geology*, 92, 1-13 (2007).
- [10] Biescas, E., Crosetto, M., Agudo, M., Monserrat, O., and Crippa, B. "Two radar interferometric approaches to monitor slow and fast land deformation", *Journal of Surveying Engineering*, 133, 66-71 (2007).
- [11] Herrera, G., Tomás, R., Lopez-Sanchez, J. M., Delgado, J., Mallorqui, J. J., Duque, S., and Mulas, J. "Advanced DInSAR analysis on mining areas: La Union case study (Murcia, SE Spain)", *Engineering Geology*, 90, 148-159 (2007).
- [12] Guéguen, Y., Deffontaines, B., Fruneau, B., Heib, M.A., de Michele, M., Raucoules, D., Guise, Y. and Planchenault, J. "Monitoring residual mining subsidence of Nord/Pas-de-Calais coal basin from differential and Persistent Scatterer Interferometry (Northern France)", *Journal of Applied Geophysics*, 69, 24-34 (2009).
- [13] Perski, Z., Hanssen, R., Wojcik, A., and Wojciechowski. "InSAR analyses of terrain deformation near the Wieliczka Salt Mine, Poland", *Engineering Geology*, 106, 58-67 (2009).
- [14] Raucoules, D., Bourguin, B., de Michele, M., Cozannet, G., Closset, L., Bremmer, C., Veldkamp, H., Tragheim, D., Bateson, L., Crosetto, M., Agudo, M., and Engdahl, M. "Validation and intercomparison of Persistent Scatterers Interferometry: PSIC4 project results", *Journal of Applied Geophysics*, 68, 335-347 (2009).
- [15] Ng, A-H. M., Ge, L., Yan, Y., Li, X. Chang, H-C., Zhang, K., and Rizos, C. "Mapping accumulated mine subsidence using small stack of SAR differential interferograms in the Southern coalfield of New South Wales, Australia". *Engineering Geology*, 115, 1-15 (2010).
- [16] Wegmuller, U., Walter, D., Spreckels, V., and Werner, C. "Nonuniform ground motion monitoring with TerraSAR-X persistent scatterer interferometry", *IEEE Transactions on Geosciences and Remote Sensing*, 48 (2), 895-904 (2010).
- [17] Jiang, L., Lin, H., Jianwei, M., Kong, B., and Wang, Y. "Potential of small-baseline SAR interferometry for monitoring land subsidence related to underground coal fires: Wuda (Northern China) case study", *Remote Sensing of Environment* 115, 257-268 (2011).
- [18] Wegmuller, U., Strozzi, T., Benecke, N., Petrat, L., Schlautmann, M., Kuchenbecker, R., Deutschmann, J., Spreckels, V., Schafer, M., Busch, W., Schade, M., Paar, W., Maly, R., Staisch, H., Hoffmann, F., and Al-

- Enezi, A. "Monitoring mining induced ground-movements using SAR interferometric techniques". Proc.of Envisat Symposium, Montreaux, Switzerland, (ESA SP-636), 5 pgs, (2007).
- [19] Woldai, T., Opliger, G., and Taranik, J. "Monitoring dewatering induced subsidence and fault reactivation using interferometric synthetic aperture radar", *International Journal of Remote Sensing*, 30 (6), 1503-1519 (2009).
- [20] Hartwig, M. E., Paradella, W. R., and Mura, J.C. "Detection and monitoring of surface motions in active mine in the Amazon region, using persistent scatterer interferometry with TerraSAR-X satellite data", *Remote Sensing*, 5, 4719-4734 (2013).
- [21] Nogueira, A.C.R. "Faciological analysis and structural aspects of the Águas Claras Formation, Central Serra dos Carajás, Pará ", Doctoral Thesis in Geology, Federal Pará University, 167 ps, original in Portuguese (1995).
- [22] Costa, M. L., Fernandez, O.J.C., and Requelme, M.E.R. "The Azul Mn deposit, Carajás: stratigraphy, mineralogy, geochemical and geological evolution", in "Characterization of the mineral deposits in mineral districts of the Amazonia", DNPM-CT/Mineral-ADIMB, 231-333, original in Portuguese (2005).
- [23] Silva, D.C.C. "Study of the geometry and kinematic of the Archean sedimentary rocks of the Igarapé Azul Mine, Carajás, Pará", Master dissertation in Geology, Federal University of Pará, 113 ps, original in Portuguese (2006).
- [24] Vale S.A. "Lithostructural and lithogeomechanical mapping of Mine1, Azul Mn Mine", Vale's internal report, 2012, 74 ps, original in Portuguese (2012).
- [25] Bieniawski, Z.T. "Engineering Rock Mass Classifications", John Wiley & Sons, New York, 272 ps (1989).
- [26] Paradella, W.R., and Cheng, P. "Using GeoEye-1 stereo data in mining application: automatic DEM generation". *GEOinformatics*, 1 (January/February): 10-12 (2013).
- [27] Vale S.A. "Geotechnical monitoring with slope stability radar: Central-North and South walls, Mine 1, Azul Mn Mine", Vale's internal report, 2012, 7 ps, original in Portuguese (2012).
- [28] Ferretti, A., Prati, C., and Rocca, F. "Permanent Scatterers in SAR Interferometry", *IEEE Transactions on Geoscience and Remote Sensing*, 39 (1): 8-20 (2001).
- [29] Werner, C., Wegmüller, U., Strozzi, T. and Wiesmann, A., "Interferometric point target analysis for deformation mapping," *Proc. IGARSS*, Toulouse, 4362–4364 (2003).
- [30] Hooper, A, Zebker, H, Segall, P, and Kampes, B. "A new method for measuring deformation on volcanoes and other natural terrains using InSAR Persistent Scatterers", *Geophysical Research Letters*, 31, L23611, (2004).
- [31] Wegmuller, U., Walter, D., Spreckels, V. and Werner, C.L., "Nonuniform ground motion monitoring with TerraSAR-X Persistent Scatterer Interferometry, *IEEE Transactions on Geoscience and Remote Sensing*, 48 (2): 897-904 (2010).
- [32] Orman, M., Peevers, R., and Sample, K. [Waste Piles and Dumps], *SME Mining Engineering Handbook*, 3rd ed., SME, Englewood, CO, USA, Vol. 1, 667–680 (2011).